



Study of global cloud droplet number concentration with A-Train satellites

S. Zeng^{1,2}, J. Riedi³, C. R. Trepte², D. M. Winker², and Y.-X. Hu²

¹Oak Ridge Associated Universities, Oak Ridge, TN, USA

²NASA Langley Research Center, Hampton, VA, USA

³Laboratoire Optique d'Atmosphérique, Université Lille 1, Villeneuve d'Ascq, France

Correspondence to: S. Zeng (shan.zeng@hotmail.com)

Received: 23 September 2013 – Published in Atmos. Chem. Phys. Discuss.: 7 November 2013

Revised: 22 May 2014 – Accepted: 29 May 2014 – Published: 16 July 2014

Abstract. Cloud droplet number concentration (CDNC) is an important microphysical property of liquid clouds that impacts radiative forcing, precipitation and is pivotal for understanding cloud–aerosol interactions. Current studies of this parameter at global scales with satellite observations are still challenging, especially because retrieval algorithms developed for passive sensors (i.e., MODerate Resolution Imaging Spectroradiometer (MODIS)/Aqua) have to rely on the assumption of cloud adiabatic growth. The active sensor component of the A-Train constellation (i.e., Cloud-Aerosol Lidar with Orthogonal Polarization (CALIOP)/CALIPSO) allows retrievals of CDNC from depolarization measurements at 532 nm. For such a case, the retrieval does not rely on the adiabatic assumption but instead must use a priori information on effective radius (r_e), which can be obtained from other passive sensors.

In this paper, r_e values obtained from MODIS/Aqua and Polarization and Directionality of the Earth Reflectance (POLDER)/PARASOL (two passive sensors, components of the A-Train) are used to constrain CDNC retrievals from CALIOP. Intercomparison of CDNC products retrieved from MODIS and CALIOP sensors is performed, and the impacts of cloud entrainment, drizzling, horizontal heterogeneity and effective radius are discussed. By analyzing the strengths and weaknesses of different retrieval techniques, this study aims to better understand global CDNC distribution and eventually determine cloud structure and atmospheric conditions in which they develop. The improved understanding of CDNC can contribute to future studies of global cloud–aerosol–precipitation interaction and parameterization of clouds in global climate models (GCMs).

1 Introduction

Cloud droplet number concentration is one of the most important cloud microphysical properties as it is intimately related to the cloud droplet size distribution, chemical composition of condensation nucleation nuclei (CCN), and the thermodynamical and dynamical state (i.e., updraft velocity, mixing rates) of the cloudy air during its formation (Seinfeld and Pandis, 1998). This property is directly linked to cloud evolution (i.e., water vapor condensation, droplet nucleation and drizzling processes), impacts cloud radiative properties and precipitation development, and it is pivotal in cloud–aerosol interactions.

Better representations of clouds and cloud–aerosol–precipitation interactions would help process modeling and improve understanding of regional/global climate changes and daily weather forecasts. Many studies have identified that aerosol–cloud interactions constitute the largest source of uncertainties in estimating radiative forcing of the earth-atmosphere system (Penner et al., 2011). For the same total cloud water content, increasing the number concentration of precursor aerosols may lead to a decrease in cloud effective radius and, therefore, to an increase in cloud albedo (i.e., the first aerosol indirect effect; Twomey, 1977). Recent research discusses whether or not the marine biosphere plays a non-negligible role in regulating cloud microphysical properties in a pristine oceanic atmosphere, and so far many studies have examined biogenic influence on cloud microphysics (Charlson et al., 1987; Lana et al., 2012; Ayers and Caine, 2007). Validation of relationships between cloud microphysics and marine biogenic aerosols that serve as CCN

can improve our understanding of the ocean–atmosphere interaction.

Until recently, studying Cloud Droplet Number concentration (CDNC) on global scales has been challenging. Field measurements provide more accurate CDNC information but their temporal and spatial coverage is limited. Satellites could provide broad sampling coverage of continuous observations; however, retrieval algorithms from passive sensors (e.g., MODerate Resolution Imaging Spectroradiometer (MODIS)/Aqua) suffer from important uncertainties because they rely heavily on assumptions regarding adiabatic or subadiabatic cloud growth. As a matter of fact, most clouds in the atmosphere do not grow adiabatically. Real clouds are predominantly subadiabatic because of warm rain process and droplet evaporation/breakup processes associated with the cloud top entrainment (Pruppacher and Lee, 1976). Therefore, it is highly relevant to investigate and understand the retrieval bias due to cloud diabatic growth. The active sensor Cloud-Aerosol Lidar with Orthogonal Polarization (CALIOP)/CALIPSO, another A-Train member, permits retrievals of CDNC from the depolarization measurement at 532 nm. This technique differs and has a weak dependence upon an adiabatic assumption. On the other hand, the CDNC retrieval methodology requires a priori information on the r_e , which cannot be derived from CALIOP. This information is retrieved independently from other sensors, such as MODIS/Aqua or POLDER/PARASOL. The CDNC retrieval accuracy, therefore, strongly depends on the accuracy of the r_e retrieved from other sensors. This calls for a careful evaluation and intercomparison of CDNC data sets derived on a global scale from passive (MODIS) and active (CALIOP) sensors based on these different retrieval techniques.

In Sect. 2, the CALIOP/CALIPSO, MODIS/Aqua and POLDER3/PARASOL data are presented, and algorithms, their theoretical basis and main characteristics are summarized. Comparison methodology of CDNC between CALIOP and MODIS and the corresponding results are given in Sect. 3. Impacts of cloud entrainment/drizzling, horizontal heterogeneity and r_e are discussed in Sect. 4, and conclusions are drawn in Sect. 5.

2 Data and algorithms

In our study, collocated data (CALTRACK data from ICARE Data and Service Centre; Zeng, 2011) from level-2 CALIOP/CALIPSO, MODIS/Aqua and POLDER3/PARASOL cloud products extracted along the CALIOP track at 5 km horizontal resolution are being considered for the period from November 2007 to December 2008. Overcast water clouds are filtered for the study with a combination of CALIOP, MODIS and POLDER cloud products. We also remove thin clouds with optical thickness of less than 5 as detected by MODIS because those thin clouds have large uncertainties when retrieving cloud optical

thickness and effective radius (Zhang et al., 2011). Hereafter, we provide a brief summary of the CDNC retrieval algorithms of CALIOP, MODIS and their theoretical basis, including their advantages and limitations.

2.1 CALIOP/CALIPSO

CALIOP (Cloud-Aerosol Lidar with Orthogonal Polarization) is an active two-wavelength polarization-sensitive lidar with a horizontal resolution of 333 m and vertical resolution of 30–60 m (Winker et al., 2003). The level-2 cloud layer products are derived at a horizontal resolution of 5 km. CALIOP uses a level-2 layer integrated depolarization ratio (δ) and collocated droplet effective radius (r_e unit: μm) from passive sensors to retrieve the CDNC (N ; unit: cm^{-3} ; see Eq. (1), corresponding to Eq. (9) in Hu et al., 2007). The retrieval sensitivity of the r_e from the CALIOP extinction and layer-integrated depolarization ratio is very low; there is no r_e product derived directly from CALIOP. Collocated r_e values retrieved from MODIS (Nakajima and King, 1990; Platnick et al., 2003) or POLDER (Bréon and Doutriaux-Boucher, 2005) are used to constrain the CDNC retrieval of CALIOP. The method is based on the fact that the total extinction (β ; unit: km^{-1}) is a sum of extinction for each single droplet (β_s ; $\beta_s = 2\pi r_e^2$). The total extinction coefficients of water clouds can be retrieved from δ and r_e ($\beta = r_e^{1/3}(1 + 135\delta^2/(1 - \delta^2))$; see Eq. (3) in Hu et al., 2007) where δ is related to multiple scatter and r_e determines the backward proportion of single scatter and absorption. Droplet number concentration is therefore the quotient of β and β_s as shown in the following equation:

$$N \approx 1000 \frac{1 + 135\delta^2/(1 - \delta^2)}{2\pi(r_e/(1 \mu\text{m}))^5/3}. \quad (1)$$

As real cloud droplets are not monodispersely distributed, the true droplet number concentration can be represented as the product of N (unit: cm^{-3}) and a factor k (see Eq. 8 in Hu et al., 2007). k is the ratio of effective radius to volume radius and is assumed constant at 0.6438 in our formula by considering a gamma distribution of the droplets with an effective variance of size distribution (v) equal to 0.13 for MODIS ($k = 1/((1-v) \times (1-2 \times v))$; Hu, et al. 2007). We used the r_e from both passive sensors (Figs. 1–6 from MODIS and Fig. 7 from POLDER) for our calculations in the following.

The main advantage of CALIOP retrieval is that an adiabatic assumption is not required for the retrieval. The CDNC can be accurately retrieved if the layer-integrated depolarization ratio and the r_e are accurate. Since collocated r_e values retrieved from MODIS or POLDER are used to constrain the CDNC retrieval of CALIOP, the retrieval accuracy depends strongly on the correctness of the r_e derived from these passive instruments. In addition, as CALIOP signal could only detect the uppermost top of clouds with $\tau < 5$ (Winker et al., 2009), the effective radius corresponding to this layer is needed to calculate the CDNC corresponding to this layer. If

CDNC is vertically constant, the retrieval can represent the true value for the whole cloud. In reality, due to cloud top entrainment, CDNCs at the cloud top are smaller than those in clouds, leading to a negative retrieval bias.

2.2 MODIS/Aqua

MODIS (MODerate Resolution Imaging Spectroradiometer) is a relatively high spatial resolution (1 km) and wide spectral (0.41–15 μm) imaging radiometer that provides global observations of atmospheric properties (Platnick et al., 2003). The level-2 cloud products are derived at a resolution of 1 km (for both cloud optical thickness and r_e) or 5 km. Inference of CDNC from MODIS uses both cloud optical thickness and droplet effective radius, which are obtained directly from a bispectral technique using bidirectional solar visible reflectance and near-infrared absorption (Nakajima and King, 1990). MODIS r_e is retrieved from three bands in the near infrared (at 1.6 μm , 2.1 μm and 3.7 μm bands). The 3.7 μm retrieval is expected to represent the droplet size closest to the cloud top (Platnick, 2000) and to be the least sensitive to the 3-D radiative bias (Zhang and Platnick, 2011), and it is therefore the best choice for the CDNC calculation.

CDNC retrievals from Eq. (2) are valid under the assumption that clouds develop in adiabatic conditions, implying that liquid water content (LWC: the sum of single water droplet mass; $\text{LWC} = N_{\text{ad}} \times 4/3\pi r_e^3 \rho_w$; ρ_w (kg m^{-3}) is water density; r_e (μm) is effective radius; N_{ad} (cm^{-3}) is droplet number concentration in clouds developed in adiabatic conditions) increases linearly with height above cloud base ($\text{LWC} = C_w \times H$; H (km) is height above clouds; C_w (kg m^{-4}) is moist adiabatic condensation rate; Benartz, 2007). In an adiabatic cloud model, cloud optical thickness (τ) is a function of N_{ad} and H ($\tau = 3/5\pi^{1/3} Q(3/4C_w/\rho_w)^{2/3}(kN_{\text{ad}})^{1/3}H^{5/3}$; Q is extinction efficiency ≈ 2 ; see Eq. (5) in Benartz, 2007). The three independent relationships above allow retrieving the three variables, N_{ad} , H and LWC. Therefore, N_{ad} is a function of τ and r_e as shown in Eq. (2). Real N in clouds developed in adiabatic and diabatic conditions is a product of N_{ad} and the degree of adiabaticity (f_{ad}). f_{ad} is in range of $0 < f_{\text{ad}} \leq 1$ and $f_{\text{ad}} = 1$ means adiabatic. It is assumed that it has a constant value of 0.8 in our calculation (Painemal and Zuidema, 2011).

$$N_{\text{ad}} \approx \frac{\sqrt{10}}{4\pi} \left[\frac{C_w \tau}{\rho_w r_e^5} \right]^{0.5} \quad (2)$$

C_w used above is defined by Grabowski (2007, see Appendix A5) and is a function of temperature (using cloud top temperature from MODIS), pressure (using cloud top pressure calculated from CALIOP cloud top altitude) and water vapor saturation pressure (using a function of T defined by Linblom and Nordell (2006); see Eq. 8). Same to Eq. (1), the true droplet number concentration is a product of N and k when a gamma distribution of the droplets is

considered. Results of deviations from this hypothesis have been investigated through comparison with the in situ observations (Painemal and Zuidema, 2011; Min et al., 2012). The MODIS CDNC values (derived with $f_{\text{ad}} = 0.8$) are quite close to in situ observations for stratocumulus over the Chile–Peru coast.

Concerning this method, the retrieval suffers from the adiabatic assumption (i.e., what the real value of f_{ad} is) and uncertainties in both τ and r_e retrievals, e.g., biases due to 3-D radiative transfer and surface reflectance. Underestimation of cloud entrainment (a smaller f_{ad}) causes positive bias for the MODIS retrieval; as mentioned above, the opposite is the case for CALIOP retrieval. As cloud entrainment increases (f_{ad} decreases), the positive bias due to the underestimation of cloud entrainment also increases. Droplet effective radius derived from MODIS tends to be larger than the true value, mostly because of neglecting cloud entrainment and horizontal photon transport (the 3-D radiative bias) within heterogeneous clouds (Zhang and Platnick, 2011). In addition to the MODIS r_e , we also investigated CALIOP CDNC retrievals using the product of the r_e and the effective variance of size distribution derived from POLDER3/PARASOL.

2.3 POLDER3/PARASOL

POLDER (Polarization and Directionality of the Earth Reflectance) is a multipolarization, multidirectional (16 directions) and multispectral (443–1020 nm) imaging radiometer with a native resolution of 6 km \times 7 km to provide global and repetitive observations of the solar radiation and polarized radiance reflected by the earth-atmosphere system (Deschamps et al., 1994). From POLDER observations, the r_e and effective variance of size distribution can be retrieved using an angular polarization signal near cloudbow directions (Bréon and Doutriaux-Boucher, 2005), which are very sensitive to the microphysical properties of droplets at the very top of clouds. Since the CALIOP signal also detects the uppermost top of clouds, POLDER r_e is relevant for use in combination with CALIOP measurements. The angular position of maxima and minima in the polarized phase function is only sensitive to r_e . This method is applicable only to homogeneous clouds with narrow size distributions, which are required to produce significant polarization supernumerary bows, on which the technique relies. Also, due to the angular sampling required to analyze the polarized phase function, the POLDER retrievals currently available are significantly coarser (200 km² \times 200 km²) than the MODIS ones. These two factors, namely the high sensitivity to narrow size distribution and the large area required to perform retrievals, can potentially also bias the r_e retrieved from POLDER in a way that might have been underestimated before. In practice, for large areas within which cloud optical thickness varies significantly, the average polarization signal will be an average of the polarized reflectance produced on smaller scales. Because polarized reflectance gets saturated rapidly compared

to total radiance, the resulting polarization signal is not a radiative weighted average of individual contribution but a simple mean. Therefore, thin clouds that tend to contribute fewer signals in total radiance measurements are in line with thicker clouds when it comes to polarization reflectance. In conclusion, although on rather small scales it is true that polarization is less subject to 3-D effects than total radiance, the fact remains that using polarized reflectance averaged over large areas can induce some nonintuitive biases. As a simple example, if we assume that thinner parts of a cloud field have a smaller r_e than thicker parts, then the r_e retrieved from polarization might be biased low compared to an r_e retrieved from a bispectral technique which is inferred from total radiance and corresponds to an r_e which, to a first order, is more weighted by total cloud water content. This type of bias could be even more important in the case of correlation between cloud optical thickness and droplet size distribution width, to which the polarization technique is very sensitive. Until higher resolution polarization measurements or retrievals can be obtained, the POLDER r_e retrievals shall not be considered free of potential biases and the above considerations shall be kept in mind when trying to draw conclusions from the comparison of POLDER and MODIS r_e and derived CDNC values. With that in mind, the POLDER r_e are found smaller than the MODIS ones, which calls for further understanding of these differences as the selection of r_e is quite critical for the accuracy of CDNC retrieved from CALIOP.

3 Results

In this section, we will show geographical distributions, seasonal variations, and the observed relationship between CALIOP and the MODIS CDNCs. Discussions about different factors that impact the CDNC retrieval are provided in the next section.

3.1 Geographical distributions of CDNC and their differences

In Fig. 1, we present geographical distributions of the CDNC derived from MODIS (a) and CALIOP (b) and their relative differences calculated as the ratio of CDNC differences (CALIOP minus MODIS) to the mean CDNC of the two sensors. In general, we see that the two sensors show similar geographical distributions of CDNC, with the MODIS values globally larger than the CALIOP ones (bar scales are different). Higher droplet number concentrations are found over land, around continents over ocean and in the storm tracks that agree with model simulations and observations of aerosols (Barahona et al., 2011; Moore et al., 2009, 2013; Vignati et al., 2010; Remer et al., 2008). However, over the open ocean, values are as low as fewer than 100 cm^{-3} for both sensors. Relative differences are smaller (close to

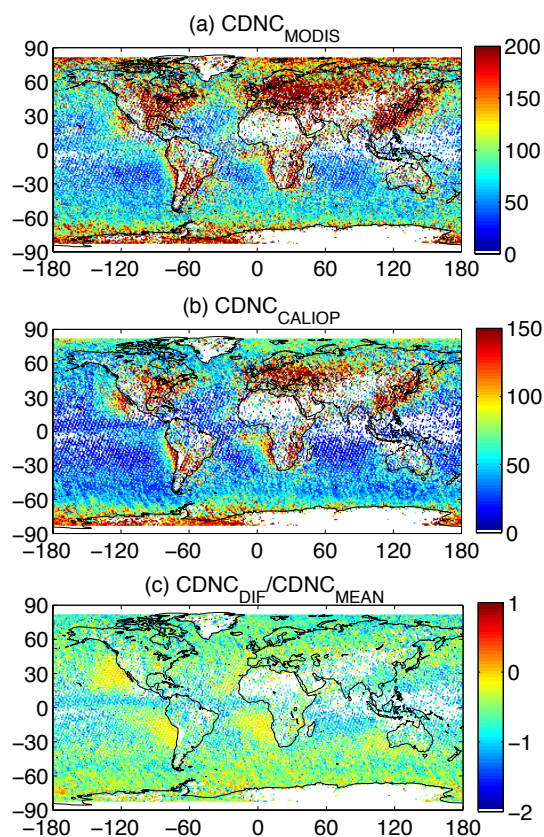


Figure 1. Geographical distributions of CDNC (cm^{-3}) derived from MODIS (a), CALIOP (b) and their relative differences (c). The MODIS $3.7\ \mu\text{m}$ effective radius is used for the calculation.

–20 %) in those regions where homogenous clouds and adiabatic conditions are known to occur, i.e., off the western coasts of continents and in the subsidence regimes of storm tracks.

3.2 Seasonal variations of CDNC

In Fig. 1, we have illustrated that MODIS and CALIOP CDNCs have similar geographical distributions. We also investigate whether they have similar seasonal variations. Figure 2 presents the geographical distributions of the correlation coefficients (a) and the slopes (b) of linear relationships of monthly MODIS and CALIOP CDNCs, and seasonal variations of MODIS (dashed line) and CALIOP (solid line) CDNCs for four specific regions (c, d, e and f). The correlation coefficients and the slopes are calculated from linear relationships (the CALIOP CDNC as a function of the MODIS one) of monthly mean CDNCs of MODIS and CALIOP (12 months counted). Seasonal variation is represented as the ratio of differences between monthly and annual mean values to the annual mean value. In Fig. 2a, we see that MODIS and CALIOP CDNCs have similar seasonal variations over the whole globe with correlation coefficients

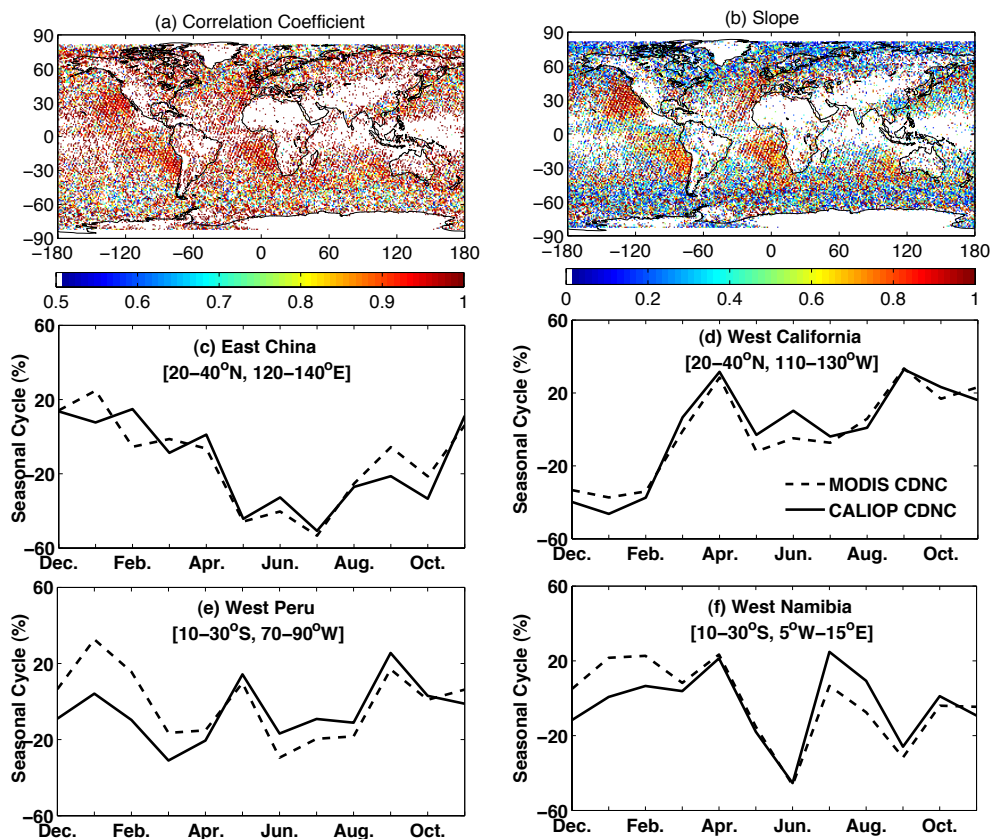


Figure 2. Geographical distributions of the correlation coefficients (a) and the slopes (b) between monthly MODIS and CALIOP CDNCs, and seasonal variations of MODIS (dashed line) and CALIOP (solid line) CDNCs for a year from December 2007 to November 2008 and for four different regions: east of China (c; regions of 20–40° N and 120–140° E), west of California (d; regions of 20–40° N and 110–130° E), west of Peru (e; regions of 10–30° S and 70–90° W) and west of Namibia (f; regions of 10–30° S and 5° W–15° E).

superior to 0.5, in particular for the regions to the west of continents where correlation coefficients are as high as more than 0.9. In Fig. 2b, we see the slopes are as high as about 0.7 in the regions to the west of continents, which means the CALIOP CDNC is about 0.7 of the MODIS one, but values are quite low in the other regions.

Seasonal cycles of CDNC show similar trends between CALIOP and MODIS for different regions (Fig. 2c, d, e and f) though they differ from region to region: to the east of China, CDNCs are higher in winter and lower in summer; to the west of California, CDNCs are higher in spring and autumn and lower in winter; to the west of Peru, CDNCs are higher in January, May and September; and to the west of Namibia, CDNCs are higher in April and July. The underlying reasons for CDNC seasonal variations will be examined in a future study that is related to seasonal changes of different CCN sources. However, this is not the objective of this paper and will not be discussed.

3.3 Relationship between MODIS and CALIOP CDNC

In Fig. 3, we present the two-dimensional relationships between the MODIS and the CALIOP CDNCs over ocean (a) and over land (b). Both linear relationships are significant ($p < 0.001$) according to Student's t test. From Fig. 3a, we clearly see that CALIOP and MODIS CDNCs are strongly correlated over ocean with a correlation coefficient as high as 0.75. The CALIOP CDNC is on average about three fourth (0.75) of the MODIS one. It supports relationships shown in Figs. 1 and 2, which indicate that, despite using very different techniques for the retrievals, CDNCs derived from the two sensors are similar to a certain degree to the MODIS values larger than the CALIOP ones. Over land, the slope (0.49) and correlation coefficient (0.53) of the two CDNCs are worse than over ocean. This may be due to fewer samples and larger uncertainties in the retrievals of r_e and τ . Over land, uncertainties from the surface reflectance dominate the errors for thinner and broken clouds (Platnick and Valero, 1995). Overall, it is still hard to determine at this stage which sensor represents the most accurate CDNC values; however, their spatial and seasonal distributions can at

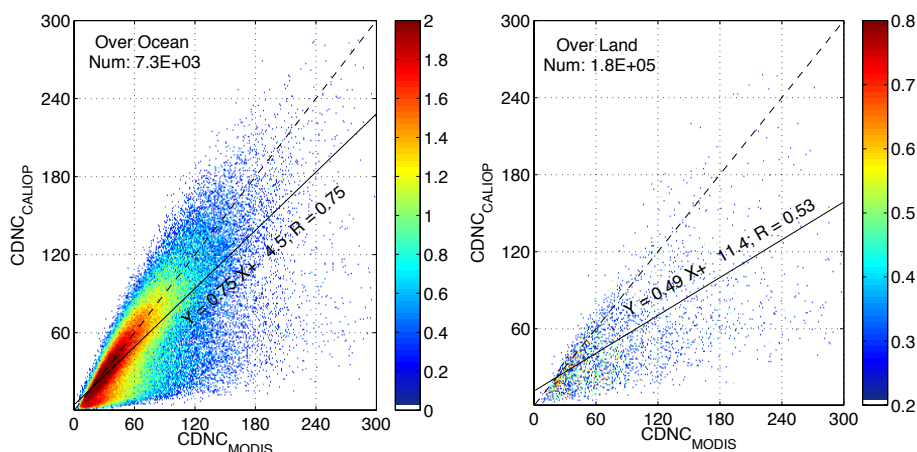


Figure 3. Relationship between the MODIS and CALIOP CDNCs over ocean (a) and over land (b). The dashed line is the $x = y$ line (x : MODIS CDNC; y : CALIOP CDNC), and the solid line is the CDNC linear regression line. The color bar represents the logarithm of the pixel number. “Num” represents pixel number and “ R ” is the correlation coefficient of the linear relationship of the two CDNCs.

least be observed consistently from both data sets. This allows us to quantitatively determine regions of highest CDNC compared to others.

4 Discussion

As was mentioned in Sect. 2, the accuracy of CDNC retrieval depends on the accuracy of the derived r_e for CALIOP and on the adiabaticity degree of the atmosphere for MODIS. In this section, we discuss possible impacts.

4.1 Impact of cloud entrainment and drizzling

Clouds in the atmosphere are predominantly subadiabatic for at least two reasons. First, entrainment of unsaturated environmental air into clouds dilutes and evaporates the droplets, leading to a decrease of r_e and CDNC at the cloud top. Second, warm rain processes, such as drizzling, also produce a decrease of r_e and CDNC at the cloud top. As mentioned in Sect. 2, the subadiabaticity can impact the retrieval of the MODIS CDNC via the degree of adiabaticity f_{ad} , and the real value would be smaller than retrieval if f_{ad} were inferior to 0.8. The stronger the cloud entrainment (smaller f_{ad}) is, the larger the retrievals are compared to the real values. Furthermore, since CDNC is not vertically constant in clouds, also because of the entrainment, the CALIOP retrieval could not be representative for the whole cloud, and is always smaller than the true value for the whole cloud. Overall, cloud adiabaticity has an impact on both the r_e and CDNC and biases the values at the cloud top in the same direction.

In Fig. 4a, we present the geographical distribution of relative r_e differences between the 3.7 μm and the 2.1 μm bands (calculated as the ratio of r_e differences ($r_{e,3.7} - r_{e,2.1}$) to the mean r_e of the two bands) from MODIS; these are the ratio

of r_e differences to r_e mean values. In theory, $r_{e,3.7}$ corresponds more closely to the effective radius at the cloud top than does $r_{e,2.1}$ (Platnick, 2000; Zhang and Platnick, 2011), and its value should be larger than $r_{e,2.1}$ according to the classic adiabatic growth model (Brenguier et al., 2000). From Fig. 4a, we find that in some well-known adiabatic and homogeneous cloud regions (i.e., in the storm tracks and to the west of continents), differences of $r_{e,3.7}$ and $r_{e,2.1}$ are close to zero or slightly positive, while in other places differences are negative. Comparing Fig. 4a to Fig. 1c, it is clear that CDNC differences and r_e differences between 2.1 μm and 3.7 μm bands show similar geographic distributions. In the storm tracks and to the west of continents, both differences are small, partially due to less subadiabatic bias (f_{ad} close to 0.8). Under extreme subadiabatic conditions in the other regions where f_{ad} is inferior to 0.8, MODIS retrieval calculated with f_{ad} equal to 0.8 is therefore larger than the real value ($N = N_{ad} \times f_{ad}$; $f_{ad} < 0.8$). However, for CALIOP, CDNC retrieval does not depend on adiabatic assumption but CDNCs at the cloud top are smaller than those in clouds. The differences between CALIOP and MODIS can to a certain extent indicate the degree of adiabaticity: larger differences appear when subadiabaticity tends to be important, while smaller differences appear when adiabatic conditions prevail.

In Fig. 4b, we show the two-dimensional histogram of the pixel number as a function of relative CDNC differences and relative r_e differences between 3.7 μm and 2.1 μm bands. We selected overcast clouds over ocean for our analysis because of fewer uncertainties on the retrievals of τ and r_e (Wolters et al., 2010; Zeng et al., 2012). From this figure, we see that most of the CDNC differences decrease when r_e differences decrease. Linear relationship is significant ($p < 0.001$) according to Student’s t test. The correlation coefficient of the linear relationship is 0.53. This means that the more important the subadiabaticity is, the larger the negative differences

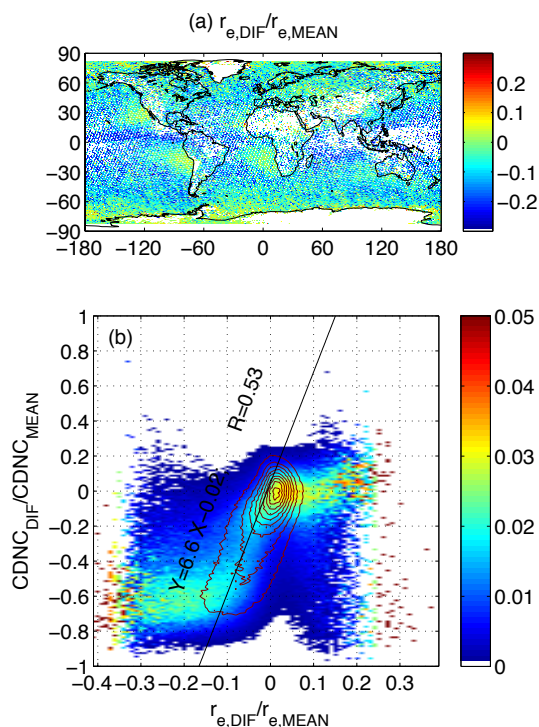


Figure 4. Geographical distribution of the relative difference of effective radius between $3.7\ \mu\text{m}$ and $2.1\ \mu\text{m}$ bands (a) and two-dimensional histogram between relative CDNC differences and relative effective radius difference between $3.7\ \mu\text{m}$ and $2.1\ \mu\text{m}$ bands (b). The color bar represents the normalized pixel number of each bin of effective radius difference. The solid straight line represents the linear relationship, and solid circle lines are isolines of the pixel number.

are between $r_{e,3.7}$ and $r_{e,2.1}$, and the larger the negative differences are between CALIOP and MODIS CDNCs (f_{ad} is smaller than 0.8). The CALIOP and MODIS CDNCs are quasi-equal when $r_{e,3.7}$ is much larger than $r_{e,2.1}$, most likely corresponding to cases of adiabatic conditions.

For further verification of adiabatic effect on the CDNC retrieval, in particular for cases of drizzling, we plot in Fig. 5 the two-dimensional histograms of relative CDNC differences against $r_{e,2.1}$ (a) and relative r_e differences against $r_{e,2.1}$ (b). The histogram is normalized for each r_e bin. According to Nakajima et al. (2010a, b), with collocated CloudSat observations, clouds with MODIS $r_{e,2.1} > 15$ are often found to be associated with drizzle. From Fig. 5, we see that both relative CDNC differences and relative r_e differences are important when $r_{e,2.1}$ is superior to 15. This suggests that increasing differences between $r_{e,2.1}$ and $r_{e,3.7}$ and between MODIS and CALIOP CDNCs with an r_e are a result of increasing drizzle probability with increasing $r_{e,2.1}$. Large droplets linked to drizzling and subadiabatic conditions could lead to more important differences between the CALIOP and MODIS CDNCs (about 0.3 of bias) compared to the differences between $r_{e,3.7}$ and $r_{e,2.1}$ (about 0.2 of bias).

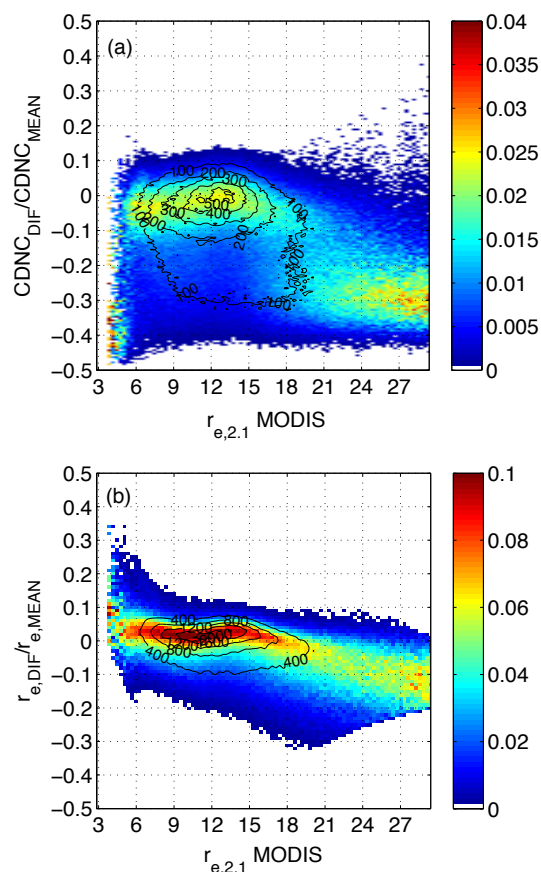


Figure 5. Two-dimensional histograms between relative CDNC differences and effective radius at $2.1\ \mu\text{m}$ bands (a) and between relative effective radius differences and effective radius at $2.1\ \mu\text{m}$ bands (b). The color bar represents the normalized pixel number of each effective radius bin. Solid circle lines are isolines of the pixel number.

4.2 Impact of 3-D radiative effect due to horizontal heterogeneity

A recent study from Zhang and Platnick (2011) has demonstrated that the $r_{e,3.7}$ and $r_{e,2.1}$ differences are not only a result of cloud entrainment and drizzling, but that they are also, to a large extent, attributable to the horizontal photon transport, namely the 3-D radiative bias caused by the plan-parallel cloud assumption in the retrieval (Zhang and Platnick, 2011; Di Girolamo, 2013). Cloud heterogeneity has a more important impact on the retrieval of $r_{e,2.1}$ than on the $r_{e,3.7}$. It has been found that the r_e derived from MODIS is slightly larger than the in situ measurements (Painemal and Zuidema, 2011). Compared to the 3-D radiative transfer models, r_e bias is about $4\text{--}6\ \mu\text{m}$ across the globe with different biases for different clouds, i.e., $1\text{--}2\ \mu\text{m}$ for less heterogeneous marine stratiform clouds and $7\text{--}12\ \mu\text{m}$ for more heterogeneous marine cumuliform clouds (Di Girolamo, 2013).

This cloud-horizontal heterogeneity can impact the CDNC retrievals mainly via the uncertainty of r_e and τ retrieval.

In Fig. 6, we selected all clouds over ocean, and plotted the two-dimensional histograms between relative CDNC differences and cloud heterogeneity (a) and between relative r_e differences and cloud heterogeneity (b). The color bar represents the normalized pixel number of each bin of cloud heterogeneity, which is represented by the ratio of the standard deviation to the mean τ derived from MODIS level-2 products into a $20 \times 20 \text{ km}^2$ grid box. The r_e differences slightly decrease with cloud heterogeneity (Fig. 6b), while the CDNC differences decrease more significantly when clouds become broken or inhomogeneous (Fig. 6a). When clouds become inhomogeneous, the retrieved r_e using a 1-D radiative transfer model is larger than the true value (Di Girolamo, 2013). According to Eqs. (1) and (2), CDNC is a $-5/3$ power function of the r_e for CALIOP and $-5/2$ power function of the r_e for MODIS. Therefore, compared to MODIS, the CALIOP-derived CDNC is smaller than the true value when r_e bias increases, resulting in a negative CDNC bias between CALIOP and MODIS that increases towards inhomogeneous clouds.

4.3 Impact of effective radius

The selection of the r_e is quite important for retrievals of CDNC from CALIOP. In Fig. 7, we show geographical distributions of CALIOP CDNC obtained by using the POLDER r_e (a) and MODIS $r_{e,3.7}$ (b), POLDER CDNC (c), and MODIS CDNC (d). Because the POLDER r_e is smaller than the MODIS one and CDNC is a $-5/3$ power function of the r_e (Eq. 2), the CALIOP CDNCs calculated using the POLDER r_e (a) are much higher than when using the MODIS $r_{e,3.7}$ (b). POLDER (c) and MODIS (d) CDNCs retrieved from Eq. (2) are almost on the same order with slightly larger CDNC for POLDER. The CALIOP CDNC can reach to about 600 cm^{-3} to the west of continents using the POLDER r_e , while the values are on the order of about 150 cm^{-3} using the MODIS $r_{e,3.7}$. Over the open oceans, the CALIOP CDNC values are on the order of about 200 cm^{-3} using the POLDER r_e and about 50 cm^{-3} using the MODIS $r_{e,3.7}$. Again, it illustrates that using a different r_e results in quite different CDNC values retrieved from CALIOP: using MODIS r_e , CDNCs are slightly lower than the values used in global climate models (GCMs), while using the POLDER r_e , these are higher than the GCM results (Barahona et al., 2011). It may suggest that the POLDER r_e represents droplets size quite close to the cloud top, which may be significantly affected by aerosols and the entrainment of dry air, or it may be less impacted by 3-D radiative effects. These could result in a smaller retrieved value of r_e corresponding to an altitude somewhat above the level contributing most of the CALIOP backscatter signal.

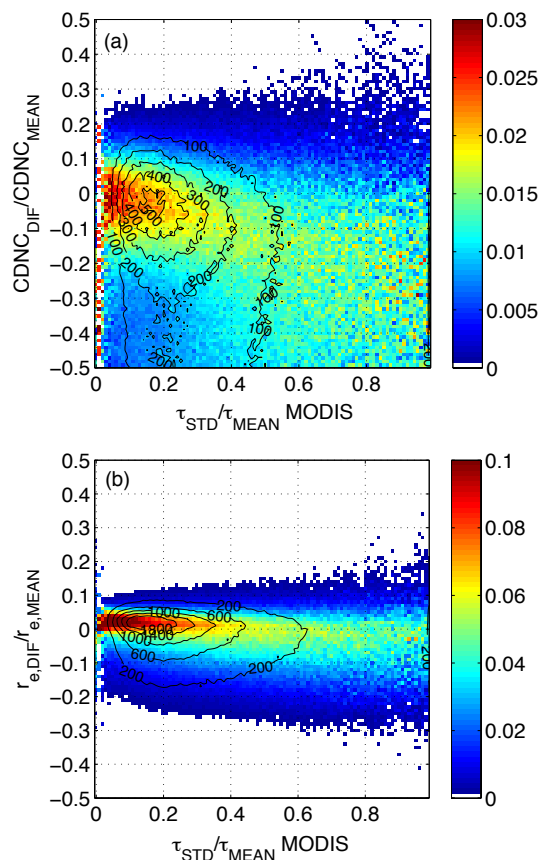


Figure 6. Two-dimensional histograms between relative CDNC differences and cloud heterogeneity (a) and between relative effective radius differences and cloud heterogeneity (b). The color bar represents the normalized pixel number of each cloud heterogeneity bin. Solid circle lines are isolines of the pixel number.

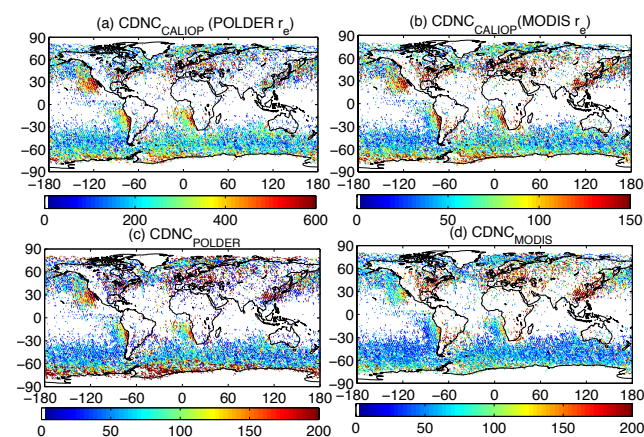


Figure 7. Geographical distributions of CALIOP CDNC (cm^{-3}) derived by using the POLDER r_e (a), MODIS $r_{e,3.7}$ (b), POLDER CDNC (c) and MODIS CDNC (d).

5 Conclusions

Cloud droplet number concentration is one of the most important key parameters of cloud microphysics. In this paper we examined their geographical distributions and seasonal variations with the MODIS and CALIOP observations. Although these two sensors use quite different techniques to retrieve CDNC, they show similar geographical distributions and seasonal variations. The CALIOP CDNCs are globally smaller than the corresponding MODIS retrievals, being about 0.75 of the MODIS values. The correlation between the two is as high as 0.75 over ocean. We discussed the possible differences from impacts of cloud entrainment/drizzling, 3-D radiative effect due to cloud horizontal heterogeneity, and selection of the r_e . As the degree of adiabaticity increases, $r_{e,3.7}$ is smaller than $r_{e,2.1}$, and the MODIS-retrieved CDNC is larger than the CALIOP one. As cloud heterogeneity increases, retrieved CDNC differences become important between CALIOP and MODIS. CALIOP has advantages in calculating CDNC at the cloud top in subadiabatic systems but its accuracy is highly controlled by the accuracy of the r_e assumption used in the algorithm. Furthermore, the retrieval of CALIOP, which is the mean value at the cloud top, may also not represent the mean values in clouds in subadiabatic systems. Using the POLDER effective r_e , retrieved CDNCs are much larger than using MODIS $r_{e,3.7}$. More accurate CDNC values from CALIOP would, in combination with MODIS, allow the study of important cloud processes such as cloud entrainment. This calls for the development of better r_e retrievals and improved description of r_e vertical profiles. Finally, the preliminary work reported indicates areas of future studies of cloud–aerosol interactions on a global scale – especially the impacts of marine biogenic aerosol on cloud microphysics.

Acknowledgements. The authors are very grateful to NASA's Langley and Goddard Centers and the French ICARE Data and Services Center for providing the CALIOP, POLDER and MODIS data used in this study. This research has been supported by NASA Postdoctoral Program.

Edited by: J.-Y. C. Chiu

References

- Ayers, G. P. and Caine, J. M.: The CLAW hypothesis: a review of the major developments, *Environ. Chem.*, 4, 366–374, 2007.
- Barahona, D., Sotiropoulou, R., and Nenes A.: Global distribution of cloud droplet number concentration, autoconversion rate, and aerosol indirect effect under diabatic droplet activation, *J. Geophys. Res.*, 116, D09203, doi:10.1029/2010JD015274, 2011.
- Benartz, R.: Global assessment of marine boundary layer cloud droplet number concentration from satellite, *J. Geophys. Res.*, 112, D02201, doi:10.1029/2006JD007547, 2007.
- Brenguier, J.-L., Pawlowska, H., Schüller, L., Preusker, R., Fischer, J., and Fouquart, Y.: Radiative properties of boundary layer clouds: Droplet effective radius versus number concentration, *J. Atmos. Sci.*, 57, 803–821, 2000.
- Bréon, F.-M. and Doutriaux-Boucher, M.: A comparison of cloud droplet radii measured from space, *IEEE Trans. Geosci. Remote*, 43, 1796–1805, 2005.
- Charlson, R. J., Lovelock, J. E., Andreae, M. O., and Warren, S. G.: Oceanic phytoplankton, atmospheric sulfur, cloud albedo and climate, *Nature*, 326, 655–661, 1987.
- Deschamps, P.-Y., Bréon, F.-M., Leroy, M., Podaire, A., Bricaud, A., Buriez, J.-C., and Sèze, G.: The POLDER mission: Instrument characteristics and scientific objectives, *IEEE Trans. Geosci. Remote*, 32, 598–615, 1994.
- Di Girolamo, L.: Cloud drop effective radius as seen from aircraft, MODIS and MISR, presented at MODIS Science Team meeting, Silver Spring, Maryland, USA, April 15–17, 2013.
- Grabowski, W. W.: Representation of Turbulent Mixing and Buoyancy Reversal in Bulk Cloud Models, *J. Atmos. Sci.*, 64, 3666–3680, 2007.
- Hu, Y., Vaughan, M., McClain, C., Behrenfeld, M., Maring, H., Anderson, D., Sun-Mack, S., Flittner, D., Huang, J., Wielicki, B., Minnis, P., Weimer, C., Trepte, C., and Kuehn, R.: Global statistics of liquid water content and effective number concentration of water clouds over ocean derived from combined CALIPSO and MODIS measurements, *Atmos. Chem. Phys.*, 7, 3353–3359, doi:10.5194/acp-7-3353-2007, 2007.
- Lana, A., Simó, R., Vallina, S. M., and Dachs, J.: Potential for a biogenic influence on cloud microphysics over the ocean: a correlation study with satellite-derived data, *Atmos. Chem. Phys.*, 12, 7977–7993, doi:10.5194/acp-12-7977-2012, 2012.
- Lindblom, J. and Nordell, B.: Water production by underground condensation of humid air, *Desalination*, 189, 248–260, 2006.
- Min, Q., Joseph, E., Lin, Y., Min, L., Yin, B., Daum, P. H., Kleinman, L. I., Wang, J., and Lee, Y.-N.: Comparison of MODIS cloud microphysical properties with in-situ measurements over the Southeast Pacific, *Atmos. Chem. Phys.*, 12, 11261–11273, doi:10.5194/acp-12-11261-2012, 2012.
- Moore, R. H., Karydis, V. A., Capps, S. L., Latham, T. L., and Nenes, A.: Droplet number uncertainties associated with CCN: an assessment using observations and a global model adjoint, *Atmos. Chem. Phys.*, 13, 4235–4251, doi:10.5194/acp-13-4235-2013, 2013.
- Moore, T. S., Campbell, J. W., and Dowell, M. D.: A class-based approach to characterizing and mapping the uncertainty of the MODIS ocean chlorophyll product, *Remote Sens. Environ.*, 113, 2424–2430, 2009.
- Nakajima, T. and King, M. D.: Determination of the optical thickness and effective radius of clouds from reflected solar radiation measurement. Part I: Theory, *J. Atmos. Sci.*, 47, 1878–1893, 1990.
- Nakajima, T., Suzuki, K., and Stephens, G.: Droplet Growth in Warm Water Clouds Observed by the A-Train. Part I: Sensitivity Analysis of the MODIS-Derived Cloud Droplet Sizes, *J. Atmos. Sci.*, 67, 1884–1896, 2010a.
- Nakajima, T., Suzuki, K., and Stephens, G.: Droplet Growth in Warm Water Clouds Observed by the A-Train. Part II: A Multisensor View, *J. Atmos. Sci.*, 67, 1897–1907, 2010b.

- Painemal, D. and Zuidema, P.: Assessment of MODIS cloud effective radius and optical thickness retrievals over the Southeast Pacific with VOCALS-REx in situ measurements, *J. Geophys. Res.*, 116, D24206, doi:10.1029/2011JD016155, 2011.
- Penner, J. E., Xu, L., and Wang, M.: Satellite methods underestimate indirect climate forcing by aerosols, *P. Natl. Acad. Sci.*, 108, 13404–13408, 2011.
- Platnick, S.: Vertical photon transport in cloud remote sensing problems, *J. Geophys. Res.*, 105, 22919–22935, 2000.
- Platnick, S. and Valero, F. P. J.: A Validation of a Satellite Cloud Retrieval during ASTEX, *J. Atmos. Sci.*, 52, 2985–3001, 1995.
- Platnick, S., King, M. D., Ackerman, S. A., Menzel, W. P., Baum, B. A., Riedi, J. C., and Frey, R. A.: The MODIS cloud products: Algorithms and examples from Terra, *IEEE Trans. Geosci. Remote*, 41, 459–473, 2003.
- Pruppacher, H. R. and Lee, I.: A comparative study of the growth of cloud drops by condensation using an air parcel model with and without entrainment, *Pure Appl. Geophys.*, 115, 523–545, 1976.
- Remer, L. A., Kleidman, R. G., Levy, R. C., Kaufman, Y. J., Tanré, D., Mattoo, S., Martins, J. V., Ichoku, C., Koren, I., Yu, H.-B., and Holben, B. N.: Global aerosol climatology from the MODIS satellite sensors, *J. Geophys. Res.*, 113, D14S07, doi:10.1029/2007jd009661, 2008.
- Seinfeld, J. H. and Pandis, S. N.: *Atmospheric chemistry and physics*, John Wiley and Sons, New York, NY, 1998.
- Twomey, S.: The Influence of Pollution on the Shortwave Albedo of Clouds, *J. Atmos. Sci.*, 34, 1149–1154, 1977.
- Vignati, E., Facchini, M. C., Rinaldi, M., Scannell, C., Ceburnis, D., Sciare, J., Kanakidou, M., Myriokefalitakis, S., Dentener, F. and O'Dowd, C. D.: Global scale emission and distribution of sea-spray aerosol: Sea-salt and organic enrichment, *Atmos. Environ.*, 44, 670–677, 2010.
- Winker, D. M., Pelon, J., and McCormick, M. P.: The CALIPSO mission: spaceborne lidar for observation of aerosols and clouds, *Proc. SPIE*, 4893, 1–11, 2003.
- Winker, D. M., Vaughan, M. A., Omar, A., Hu, Y.-X., Powell, K. A., Liu, Z., Hunt, W. H., and Young, S. A.: Overview of the CALIPSO Mission and CALIOP Data Processing Algorithms, *J. Atmos. Ocean. Tech.*, 26, 2310–2323, 2009.
- Wolters, E. L. A., Deneke, H. M., van den Hurk, B. J. J. M., Meirink, J. F., and Roebeling, R. A.: Broken and inhomogeneous cloud impact on satellite cloud particle effective radius and cloud-phase retrievals, *J. Geophys. Res.*, 115, D10214, doi:10.1029/2009JD012205, 2010.
- Zeng, S.: Comparison and statistical analysis of cloud properties derived from POLDER and MODIS instruments into the framework of the A-Train spatial experiment, Ph.D. thesis, University Lille1, Villeneuve d'Ascq, France, 2011.
- Zeng, S., Cornet, C., Parol, F., Riedi, J., and Thieuleux, F.: A better understanding of cloud optical thickness derived from the passive sensors MODIS/AQUA and POLDER/PARASOL in the A-Train constellation, *Atmos. Chem. Phys.*, 12, 11245–11259, doi:10.5194/acp-12-11245-2012, 2012.
- Zhang, Z. and Platnick, S.: An assessment of differences between cloud effective particle radius retrievals for marine water clouds from three MODIS spectral bands, *J. Geophys. Res.*, 116, D20215, doi:10.1029/2011JD016216, 2011.